NASA Technical Memorandum 87339

Concepts for Interrelating Ultrasonic Attenuation, Microstructure, and Fracture Toughness in Polycrystalline Solids

Alex Vary
Lewis Research Center
Cleveland, Ohio

May 1986

NASA

CONCEPTS FOR INTERRELATING ULTRASONIC ATTENUATION, MICROSTRUCTURE, AND FRACTURE TOUGHNESS IN POLYCRYSTALLINE SOLIDS

by

Alex Vary
National Aeronautics and Space Administration
Lewis Research Center
Cleveland, Ohio 44135

ABSTRACT

Conceptual models are advanced for explaining and predicting empirical correlations found between ultrasonic measurements and fracture toughness of polycrystalline solids. The models lead to insights concerning microstructural factors governing fracture processes and associated stress wave interactions. Analysis of the empirical correlations suggested by the models indicates that, in addition to grain size and shape, grain boundary reflections, elastic anisotropy, and dislocation damping are factors that underly both fracture toughness and ultrasonic attenuation. One outcome is that ultrasonic attenuation can predict the size of crack blunting or process zones that develop in the vicinity active cracks in metals. This forms a basis for ultrasonic ranking according to variations in fracture toughness.

E-3086

INTRODUCTION

Ultrasonic methodology for determining the fracture toughness of structural materials is of high interest. A major incentive is the need for rapid, inexpensive, and nondestructive methods for verifying fracture toughness and related mechanical properties prior to placing critical parts in service and after the parts have been exposed to service. The viability of ultrasonics for verifying fracture toughness of materials and components is being investigated. Thus far, correlations of ultrasonic measurements with toughness have been demonstrated only on a limited number of laboratory samples of polycrystalline solids. One purpose of this report is to show the

potentials of further work that is needed to establish underlying principles and appropriate approaches for applications to a variety of materials and hardware configurations.

Fracture toughness is an extrinsic mechanical property that measures a material's fracture resistance. It is the stress intensity at which a crack becomes unstable and grows catastrophically (Brown and Srawley, 1966; Hahn, et al., 1972; Kanninen and Popelar, 1985). It is known that fracture toughness is governed by microstructure and morphology in polycrystalline solids. Because the attenuation of ultrasonic waves is also governed by similar factors, one should expect correlations between toughness and ultrasonic properties of polycrystallines.

Prior works have presented empirical evidence of correlations between ultrasonic attenuation measurements and fracture toughness in polycrystalline solids (Vary, 1978; Vary and Hull, 1982, 1983). A theoretical basis has been suggested for the correlations found between ultrasonic attenuation and fracture toughness (Vary, 1979a). This paper describes some conceptual foundations that can help explain and predict the empirical correlations.

PRELIMINARY CONSIDERATIONS

Microstructural Factors

The role of microstructure in governing the mechanical properties and behavior of engineering solids is well established (Green, 1973; MacCrone, 1977; Froes, et al., 1978). Ultrasonic evaluation of mechanical properties depends on the characterization of microstructure. Figures 1 and 2 illustrate examples of the dependence of ultrasonic attenuation and fracture toughness on microstructure. Inferences of material properties are often based on metallographic and other destructive methods that reveal material composition, microstructure, and morphology. Ultrasonic methods are alternatives to the conventional approaches for characterizing microstructure and morphology.

By examining the micrographs in Fig. 1, one might infer that decreasing grain size corresponds to increasing toughness. The micrographs in Fig. 2 illustrate an opposite case where increasing grain (tungsten carbide crystal) size corresponds to increasing toughness. But, this apparent correlation with grain size is deceptive because it is the volume of cobalt "cement" (between the carbide crystals) with its high dislocation density that actually governs the fracture toughness. Clearly, there is more to consider than grain size (or even grain shape and aspect ratio) in identifying factors that govern toughness. It will be seen that ultrasonic interrogation supplements the information appearing in photomicrographs and can add to our understanding of factors that govern dynamic fracture behavior.

Ultrasonic Approach

Herein, the pulse-echo method is taken as the basis for quantitative characterization of microstructure via attenuation measurements (Papadakis, 1976; Vary, 1980). A pulse-echo system in which a single probe serves as a sending and receiving transducer to excite and collect ultrasonic signals is shown in Fig. 3. Coupling a probe to a material sample results in a series of ultrasonic echoes that can be analyzed either in the time or frequency domain, Fig. 4.

The first two echoes B_1 and B_2 in Fig. 4 are selected for measurement of energy loss due to various attenuation mechanisms. The signals are transformed to the frequency domain using digital Fourier transform algorithms (Bracewell, 1978; Vary, 1979b, 1980b; Fitting and Adler, 1981). Information concerning the material microstructure is obtained by deconvolution of waveforms B_1 and B_2 to obtain attenuation as a function of frequency. The frequency domain approach, associated concepts, and some salient results will be discussed in this paper.

CONCEPTUAL FOUNDATIONS

General

Quantitative ultrasonic characterization of mechanical properties is a relatively new and essentially unexplored area. Established foundations for observed interrelations among ultrasonic propagation, microstructure, and mechanical properties are lacking.

We will begin by considering hypothetical stress wave interactions with microstructural features during crack nucleation events at the onset of fracture. Stress waves are elastic waves that arise during dislocation movements, microcrack nucleation, plastic deformation, and fracture (Kolsky, 1963; 1973). Stress waves are ultrasonic in nature although they may exhibit audible acoustic emission components. With ultrasonic probing we expect to identify microstructural features that govern stress wave propagation and interactions during the aforementioned processes. This idea, illustrated in Fig. 5, will be pursued by using three complementary concepts: (1) a stress wave interaction concept, (2) a microstructure transfer function concept, and (3) a microcrack nucleation mechanics concept. Models based on these concepts are diagrammed in Figs. 6 to 8. The models are used to derive expressions for explaining and predicting empirical correlations that have been found among ultrasonic attenuation measurements, microstructure, and fracture toughness.

Stress Wave Interaction (SWI) Concept

The stress wave interaction (SWI) concept helps explain the correlations found between ultrasonic attenuation and fracture toughness. Experimental evidence indicates that the stress wave attenuation properties of polycrystalline metals determine toughness (Vary, 1978; Vary and Hull, 1982). Moreover, Green and his colleagues have produced experimental evidence that ultrasonic stress waves can interact with material microstructure to the

degree that they actually promote plastic deformation (Sachse and Green, 1970; Green, 1975; Green, 1981; Mignogna and Green, 1982; Green, 1986).

According to the SWI concept spontaneous ultrasonic stress waves produced during crack initiation interact with microstructural features ahead of a crack front (Vary, 1979a; 1980b). The consequent stress wave energy losses can reappear in the formation of fresh surfaces (e.g., as further cracking) (Kolsky, 1963, 1973). Or, the stress wave energy simply dissipates in dislocation motions during the formation of a crack blunting zone (Hahn et al., 1972). In the former case, stress wave interactions promote crack nucleation (e.g., grain cleavage), coalescence, and growth. In the latter case, cracking is inhibited by localized plastic deformation. Some combination of both cases is undoubtedly involved in the dynamics that underlie the fracture behavior and the fracture toughness exhibited by many engineering solids (Curran, et al., 1977; Fu, 1983a, 1983b).

In the crack nucleation version of the SWI, critical sites are activated by the spontaneous stress waves emitted at the onset of crack growth. Stress wave energy added to the local strain energy field around potential microcrack nucleation sites may result in the release of additional stress wave energy that acts on adjacent sites. The sites can be brittle grains, inclusions, or second phase particles that absorb and then release energy by breaking apart. If the advancing stress wavefront is reinforced by energy released by nucleation sites then, as indicated in Fig. 6, an avalanch (or cascading) effect may occur in which increasing numbers of crack nucleations sites are activated by the stress wavefront. Absorption of energy depends on the bandwidth of the stress wave and the presence of critical (i.e., resonant) wavelengths that are commensurate with the dimensions of potential microcrack nucleation sites.

In the crack blunting version of SWI microcrack formation is inhibited by localized containment and dissipation of stress wave energy. Solids containing grains (i.e., crystallites) with high dislocation densities exhibit higher attenuation. In this case the absorption of ultrasonic stress wave energy via dislocation motion reduces the relative amount of energy available for crack nucleation. Therefore, a greater initial stress intensity is required to produce dislocation pile-ups and consequent crack growth. The relative energy absorption by dislocation motions (damping) depends on the stress wave bandwidth (i.e., content of wavelengths that interact with dislocations).

Microstructure Transfer Function (MTF) Concept

Underlying the microstructure transfer function (MTF) concept is the hypothesis that the propagation of probe ultrasound is governed by the same microstructural factors that govern the propagation of stress waves generated during fracture initiation. There is a tacit assumption that attenuation properties measured with (low amplitude) probe ultrasound govern (high amplitude) stress waves, at least at the onset of fracture.

Specification of the magnitudes of attenuation and energy transmission during stress wave interactions requires the definition of an appropriate MTF model. In particular the MTF model must specify how stress wave energy varies with ultrasonic wavelengths (i.e., with frequency). Accordingly, considering material microstructure as mechanical "filters" that have a transfer function definable in terms of frequency dependent ultrasonic attenuation mechanisms proves to be a useful concept (Vary, 1980b; Vary and Kautz, 1986).

The conditions under which a MTF can be defined are restricted: The sample should have flat, parallel opposing surfaces and satisfy the conditions necessary to obtain two back surface echoes as shown in Figs. 4 and 7. These constraints are for mathematical convenience and also for ease of signal

acquisition (Truell et al., 1969). Signal acquisition and processing may be accomplished as described in Vary (1979b) and Generazio (1985). A polycrystalline solid is assumed for the purposes of the ensuing discussion.

The ultrasonic probe acting as sender and receiver, Fig. 4, produces a broadband pulse and a series of back surface echoes in the material specimen. The first two back echoes, B_1 and B_2, Fig. 7, are defined in terms of the internal signals I_1 and I_2 and R, the reflection coefficient at the specimen-transducer interface (Papadakis, 1976). The reflection coefficient is unity, 1, at the free surface.

$$B_1 = (1 + R)I_1 \tag{1}$$

$$B_2 = TR(1 + R)I_1 \tag{2}$$

The quantities B_1, B_2, I_1, I_2, and R, in Fig. 7, are Fourier transforms of the corresponding time domain quantities (Bracewell, 1978). The quantity T, a function of the material microstructure, is to be determined. Combining Eqs. (1) and (2) allows expressing T as the deconvolution of B_2 and B_1,

$$T = \frac{B_2}{RB_1} \tag{3}$$

The quantity T is the MTF and is assumed to incorporate effects of microstructural factors that govern stress wave attenuation in polycrystallines (e.g., grain scattering, absorption) (Serabian and Williams, 1978; Serabian, 1980). We seek a definition of T such that stress wave energy loss may be expressed in terms of an attenuation coefficient, α, in the form $E_x = E_0 \exp(-x\alpha)$, where $E_x - E_0$ is the energy loss over distance x.

Papadakis (1976) has experimentally demonstrated that the attenuation coefficient α for broadband probe ultrasound can be found by frequency spectrum analysis and expressed as

$$\alpha = \left(\frac{1}{2x}\right) \ln\left(\frac{RB_1}{B_2}\right) \tag{4}$$

Combining Eqs. (3) and (4) we have,

$$\alpha = \left(\frac{1}{2x}\right) \ln\left(\frac{1}{T}\right) \tag{5}$$

where, x is the specimen thickness indicated in Fig. 7.

An expression for α for polycrystalline solids in terms of the transfer function T based on an MTF model derived by Vary and Kautz (1986) is,

$$\alpha = \left(\frac{1}{a}\right) \ln\left(1 - G\left\{\frac{(\pi uf)^2}{1 + (\pi uf)^2}\right\}\right) + \left(\frac{h}{v}\right) f + \left(\frac{16\ K}{3a}\right) \left\{\frac{(\pi uf)^2}{1 + (\pi uf)^2}\right\}^2 \tag{6}$$

where, a is mean grain size, f is ultrasonic frequency, G is grain boundary reflection coefficient, h is damping constant, K is elastic anisotropy, u is mean grain time constant, v is ultrasonic velocity, and $u = a/v$. It will be seen that Eq. (6) forms a basis for identifying microstructural factors that govern toughness.

Use of analytical expressions of the form of Eq. (6) requires a priori knowledge of the equantities a, G, h, and K. An alternative expression for the attenuation coefficient that does not require explicit values for these quantities is desirable. One such expression that is useful for fitting experimental data is (Vary, 1979a, 1980a),

$$\alpha = cf^m \qquad f_1 < f < f_2 \ , \tag{7}$$

Equation (7) has been found to accurately represent data within the frequency range from f_1 to f_2, where attenuation is due primarily to Rayleigh scattering (Vary and Kautz, 1986). It will be seen later that the empirical constants c and m can be used to determine values for G, h, and K and that Eq. (7) forms a basis for demonstrating empirical correlations between toughness and ultrasonic attenuation while Eq. (6) provides a means for analyzing the correlations.

Microcrack Nucleation Mechanics (MNM) Concept

The microcrack nucleation mechanics (MNM) concept combines the SWI and MTF concepts in the derivation of a relation among the attenuation properties of a microstructure, stress wave sources, and potential crack nucleation sites. The MNM concept is used to account for energy dissipation between stress wave sources and potential microcrack nucleation sites (Vary, 1979a; Fu, 1982, 1983a, 1983b). Experimental evidence of ultrasonic stress wave energy dissipation leading to plastic deformation (Sachse and Green, 1970; Green, 1981; Mignogna and Green, 1982; Green, 1986) suggests the existence of stress wave energy transfer mechanisms that lead to dislocation motions and microcrack nucleations. This section describes a microcrack nucleation model from which it is possible to derive an expression relating ultrasonic attenuation and toughness.

The MNM model depicted in Fig. 8 assumes that stress wave interactions promote microcrack nucleation in accordance with the SWI concept. A stress wavefront is shown traveling from grain $\mathscr{S}$ to grain $\mathscr{R}$. These "grains" represent critical, interacting microstructural features such that, when grain $\mathscr{S}$ releases energy by fracturing, grain $\mathscr{R}$ will absorb some of this energy. Given an existing static stress field around $\mathscr{R}$, it is only necessary for the impinging stress wave to impart enough energy to take $\mathscr{R}$ above a fracture threshold. The energy imparted to $\mathscr{R}$ depends on the ultrasonic stress wave attenuating properties of the ligament between grains $\mathscr{S}$ and $\mathscr{R}$.

The MNM model depicted in Fig. 8 was applied specifically to plane strain fracture toughness data (Brown and Srawley, 1966) to derive an expression connecting ultrasonic factors and the fracture toughness quantity (K_{Ic}/σ_y) (Vary, 1979a),

$$\left(\frac{K_{Ic}}{\sigma_y}\right)^2 = M\sqrt{\frac{v_\ell \beta_\delta}{m}} \tag{8}$$

where K_{Ic} is plane strain fracture toughness and σ_y is yield strength. The right hand side of Eq. (8) consists of ultrasonically determined quantities, where v_ℓ is velocity, M is an experimental constant for the material being evaluated, and m is the exponent on frequency in Eq. (7). The quantity β_δ in Eq. (8) is the derivative

$$\beta_\delta = \left.\frac{d\alpha}{df}\right|_{f_\delta} = mc\left(\frac{v_\ell}{\delta}\right)^{m-1} \tag{9}$$

where, $d\alpha/df$ is evaluated at a frequency, $f_\delta = v_\ell/\delta$, that corresponds to a "critical" ultrasonic wavelength, λ_c, in the material. This wavelength is defined by the critical dimension, δ, in the microstructure (e.g., mean grain size or other feature that dominates during crack nucleation). This dimension is taken as the average for all microcrack nucleation sites that interact with the stress waves in accordance with the SWI concept. The critical dimension links the material transfer function, T, to specific microstructural features that govern fracture toughness.

The quantity $(K_{Ic}/\sigma_y)^2$ on the left side of Eq. (8) is termed the "characteristic length." This characteristic length quantity is also a measure of the fracture toughness (Brown and Srawley, 1966; Hahn et al., 1972). It is proportional to the size of the microcrack blunting zone that develops at the crack tip due to dislocation motions during the onset of crack growth in materials with plastic yield.

Equation (8) relates factors that govern toughness with ultrasonic propagation properties of the microstructure and predicts that the characteristic length or crack blunting zone size will be determined primarily by the attenuation properties associated with dislocation interactions.

Materials that develop larger crack blunting zones confine and absorb more stress wave energy locally and exhibit greater fracture toughness.

All the quantities in Eq. (8) are functions of material microstructure. Although the parameter M may remain essentially constant for a given alloy, the characteristic length and ultrasonic quantities (e.g., c and m in Eq. (7) and a, G, h, K, v in Eq. (6)) will change with heat treatment, phase composition, and other factors that affect toughness.

VERIFICATION AND ANALYSIS

Experimental Correlations

The correlation predicted by Eq. (8) has been experimentally verified (Vary, 1978; 1979a) and Fig. 9 shows the predicted correlation for three metals (two maraging steels and a titanium alloy). In these metals the critical microstructural dimension is the average grain size (or the subgrain "lath" spacing in the 200 grade maraging steel). The experimental data for $(K_{Ic}/\sigma_{0.2})^2$ versus $v_\ell\beta_\delta/m$ plotted in Fig. 9 were fitted by linear regression. The curve for the 200 and 250 grade maraging steels is given by

$$\left(\frac{K_{Ic}}{\sigma_{0.2}}\right)^2 = 8.34\text{x}10^{-3}\left(\frac{v_\ell\beta_\delta}{m}\right)^{0.522}$$

while for the titanium alloy the curve is given by

$$\left(\frac{K_{Ic}}{\sigma_{0.2}}\right)^2 = 1.45\text{x}10^{-2}\left(\frac{v_\ell\beta_\delta}{m}\right)^{0.564}$$

where, $\sigma_{0.2}$ is yield strength, σ_y, at 0.2 percent offset.

In the case of the titanium alloy described by Vary and Hull (1982) there are three levels of microstructure: (prior) grains, colonies (within grains), and (within colonies) alternating alpha/beta phase platelets. The question regarding which of these features exerts the greatest influence on fracture

toughness has been answered on the basis of the previously described concepts. The results shown in Fig. 10 indicate that the best empirical correlation and also the best agreement with theory (i.e., with Eq. (8)) occur with data based on the beta phase thickness (Vary and Hull, 1982). The alpha phase thickness was found to be somewhat less significant than the beta phase thickness (e.g., correlation coefficients were 0.977, and 0.998, respectively). The colony size was weakly influential, while grain size influence was indeterminate. The empirical equations for the alpha and beta phases determined by regression analysis are, respectively,

$$\left(\frac{K_{Ic}}{\sigma_{0.2}}\right)^2 = 5.91\times10^{-4}\left(\frac{v_\ell \beta_\delta}{m}\right)^{0.73}$$

$$\left(\frac{K_{Ic}}{\sigma_{0.2}}\right)^2 = 7.63\times10^{-2}\left(\frac{v_\ell \beta_\delta}{m}\right)^{0.56}$$

For the titanium alloy both the alpha and beta phases appear to be comparably critical microstructural features. Fractographic studies identify the alpha phase aspect ratio as a critical factor. The alpha platelets appear to act as obstacles to microcrack extension and dissipate energy by making the crack path tortuous via frequent, abrupt changes in direction (Froes et al., 1978). However, the best correlation coefficient for Eq. (8) is obtained with the beta phase. From an ultrasonic viewpoint the beta phase has the greatest influence on toughness. This is undoubtedly due to its greater dislocation density (about tenfold greater than the alpha phase) and concomittantly greater attenuation and greater absorption and dissipation of stress wave energy.

Analysis

Equation (6) provides a basis for analyzing the correlations in Figs. 9 and 11. First, note that the quantity $v_\ell \beta_\delta / m$ in Eq. (8) is equivalent

to the product of the size of the critical microstructural feature, δ, and the attenuation coefficient, α_δ, evaluated at the frequency corresponding to the critical wavelength δ, that is,

$$\delta\alpha_\delta = \left(\frac{v}{m}\right)\beta_\delta = vc\left(\frac{v}{\delta}\right)^{m-1} = \delta c(f_\delta)^m \tag{10}$$

where, v is taken as longitudinal velocity v_ℓ. Setting $\delta = a$ and recalling that $u_\delta = a/v = \delta/v$ and $f_\delta = v/a = v/\delta$, Eq. (6) is rearranged to get

$$\delta\alpha_\delta = -\ell n(1 - GF_\delta) + h + \frac{16}{3} KF_\delta^2 \tag{11}$$

where

$$F_\delta = \frac{(\pi u_\delta f_\delta)^2}{1 + (\pi u_\delta f_\delta)^2}$$

The quantity $\delta\alpha_\delta$ is the specific attenuation coefficient for the critical microstructural feature. And since $u_\delta f_\delta = 1$, $F_\delta = \pi^2/[1 + \pi^2]$. F_δ is a numerical factor that depends on the grain size distribution function which in the present case is taken as a log normal distribution function typical of polycrystalline solids (Vary and Kautz, 1986). Combining Eqs. (8), (10), and (11) we have

$$\left(\frac{K_{Ic}}{\sigma_y}\right)^2 = M\sqrt{-\ell n(1 - GF_\delta) + h + \frac{16}{3} KF_\delta^2} \tag{12}$$

As might be expected, characteristic length (toughness) is a function of G, h, and K, the boundary reflection, damping, and elastic anisotropy factors, respectively. In Eq. (12) fracture toughness is independent of explicit grain size, velocity, and frequency because it is defined in terms of the attenuation properties of a critical microstructural feature.

The expression on the right-hand side of either Eqs. (11) or (12) will be the same for any arbitrary dimension used for a in evaluating the quantity $a\alpha_a$. However, the factor F_δ will vary according to the spatial distribution function of the microstructural feature it represents. The factor F_δ may be invariant for homomorphic changes in the grain structure of polycrystallines (Vary and Kautz, 1986).

Insight into the quantitative effects of variations in G, h, and K can be gained by examining interrelations with the empirical parameters c and m in Eq. (7). It has been found that c and m are interdependent for variously conditioned samples of a polycrystalline material. As an example, experimentally determined values for c and m are plotted and tabulated in Fig. 11. Apparently, the parameters c and m will be interdependent for samples of a material that have undergone heat treatment or other thermomechanical processing that preserves global microstructural patterns while altering mechanical properties like toughness.

A graphical method for evaluating the quantities G, h, and K in terms of c and m was devised (Vary and Kautz, 1986). By varying a, G, h, K, and v in Eq. (6) over a range of representative values, the c and m parameters for a bounded frequency range (e.g., the Rayleigh frequencies) may be computed with Eq. (7). The parametric fields in Fig. 12 were generated by assuming a range of values for a, G, h, and K and $v = 0.55$ cm/μs corresponding to a 250 grade maraging steel (250MS). Coplotted in Fig. 12 are data for the 250MS from Fig. 11. In Fig. 12(a) the data fall near the curve for mean grain size equal to 10 μm, since $8.5 \leq a \leq 13$ μm. In Figs. 12(a) and (c) $a = 10$ μm is assumed and in Fig. 12(b) the data lie on the $G = 0.007$ curve while in Fig. 12(c) they lie near the $h = 2\times10^{-5}$ curve.

All the fields in Fig. 12 indicate that the elastic anisotropy, K, varies by roughly a half order of magnitude between the two pairs of 250MS data

points. This is significant because the left-hand pair at $m \cong 2.6$ share an average toughness $K_{Ic} = 118$ MPa$\sqrt{m}$ (megapascals square root meters) while the right-hand pair at $m \cong 3.0$ share an average toughness $K_{Ic} = 143$ MPa$\sqrt{m}$. All four 250MS samples had the same yield strength of $\sigma_y = 1400$ MPa (Vary, 1978). Apparently, the thermal treatment that increased fracture toughness from roughly 118 to 143 MPa$\sqrt{m}$ also produced an increase in elastic anisotropy of roughly a half order of magnitude in the interval between $K = 0.007$ to 0.07. This increase in K can account for an increase in (stress wave) attenuation and, hence, the correlation between attenuation and fracture toughness predicted by the conceptual models.

We note that $(K_{Ic}/\sigma_y)^2$ is also directly proportional to the damping constant, an intrinsic property of crystallites (grains) that is related to their dislocation densities (Nowick and Berry, 1972). However, in Fig. 12 the prominent increase in K, the elastic anisotropy factor, overshadows a concomitant increase in h, the dislocation damping factor, that probably contributed to the increased toughness between the two pairs of 250MS data points. The scale of Fig. 12(c) obscures the fact that the two data pairs lie near h-curves that differ by perhaps a half order of magnitude.

Since in the case of the 250MS yield strength is constant at 1400 MPa, according to Eq. (12) the increase in toughness should be proportional to the increase in G, h, or K, whichever is greatest (e.g., $(K_{Ic})^2 \approx \sqrt{K}$). Accordingly, the increase in K of between a factor of 2 and 3 inferrable from Fig. 12 predicts a corresponding increase in K_{Ic} of between a factor of approximately 1.2 and 1.3. These ratios bracket the average increase in K_{Ic} by a factor of 1.2 in the interval between the two pairs of 250MS data points. A similar argument would show a comparable change in K_{Ic} by considering the change in h for the two pairs of data points.

DISCUSSION

The preceding analysis shows that, in addition to grain size and shape, grain boundary reflections, elastic anisotropy, and dislocation damping are among factors that determine the toughness of polycrystalline solids. The SWI, MTF, and MNM concepts seem to be supported by the currently available experimental results.

Of course, it is not surprising that in polycrystallines with mobile dislocations local plastic deformations determine toughness via crack blunting (Kanninen and Popelar, 1985). The new information inferrable from Figs. 9 to 12 and from Eqs. (8) to (12) is that metals that are more attenuating tend to develop larger crack blunting zones in the vicinity of active cracks. According to Eqs. (11) and (12) the specific attenuation and the characteristic length (i.e., size of the blunting zone) are functions of the same microstructural factors. The extrinsic properties of fracture toughness and stress wave attenuation both ultimately depend on dislocation densities. Tougher metals are apparently those in which more stress wave energy transmission is impeded at grain boundaries by reflections and elastic scattering and then dissipated in localized plastic deformation zones by dislocation motions.

The preceding observations should be contrasted with experimental findings for fiber reinforced composites. In fiber reinforced plastics greater strength (and probably toughness) correspond to less attenuation (Vary and Bowles, 1977; Vary and Lark, 1979). Many composites have resin matrixes that cannot sustain plastic deformation although stress wave energy may be absorbed by matrix crazing. In this case it is better to have prompt, efficient transmission of stress wave energy away from crack nucleation sites.

In contrast with metals it is preferable for composites and similar materials with brittle matrices to exhibit lower attenuation and less

localized concentration of stress wave energy. This criterion would certainly apply to monolithic ceramics which lack plastic deformation energy absorption mechanisms such as dislocation production and movement mechanisms. The criterion might also apply to transformation toughened and fiber reinforced composite ceramics wherein energy absorption mechanisms are likely to be rapidly exhausted in the vicinity of crack fronts.

Understanding of micromechanical processes during cracking is essential (Kanninen and Popelar, 1985), especially in the case of composite materials. The formulation of Eq. (8) depended in part on an intuitive description of stress wave energy partitioning during micromechanical failure processes in polycrystalline solids (Vary, 1979a). One of the points of this paper is to indicate that advancements in nondestructive ultrasonic assessment of fracture toughness depend on advancements in fracture mechanics in the area of microcrack nucleation mechanics.

CONCLUSION

Three conceptual models interrelating ultrasonic attenuation, microstructure, and fracture toughness in polycrystalline solids were described: (1) a stress wave interaction model, (2) a microstructure transfer function model, and (3) a microcrack nucleation mechanics model. These conceptual models seem to form consistent and valid bases for explaining and predicting the experimental correlations found between ultrasonic attenuation and fracture toughness and also for identifying microstructural factors that underly the stress wave attenuation and associated toughness properties of polycrystalline solids. Analysis of the empirical correlations indicated that, in addition to grain size and shape, grain boundary reflections, elastic anisotropy, and dislocation damping are factors that underly both fracture toughness and ultrasonic attenuation. One outcome is that ultrasonic attenuation can predict the size of crack blunting or process zones that

develop in the vicinity active cracks in metals. This forms a basis for ultrasonic ranking of metals according to their fracture toughness.

REFERENCES

1. Bracewell, R.N.: The Fourier Transform and Its Applications, 2nd ed., McGraw-Hill, 1978.
2. Brown, W.F., Jr.; and Srawley, J.E.: Plane Strain Crack Toughness Testing of High Strength Metallic Materials. ASTM STP-410, American Society for Testing and Materials, Philadelphia, 1966.
3. Curran, D.R.; Seaman, L.; and Shockey, D.A.: Dynamic Failure in Solids. Phys. Today, vol. 30, no. 1, Jan. 1977, pp. 46-55.
4. Fitting, D.W.; and Adler, L.: Ultrasonic Spectral Analysis for Nondestructive Evaluation. Plenum Press, 1981.
5. Froes, F.H., et al.: Relationship of Fracture Toughness and Ductility to Microstructure and Fractographic Features in Advanced Deep Hardenable Titanium Alloys. Toughness and Fracture Behavior of Titanium, ASTM STP-651, R.G. Broadwell and C.F. Hickey, Jr., eds., American Society for Testing and Materials, 1978, pp. 115-153.
6. Fu, L.S.: Mechanics Aspects of NDE by Sound and Ultrasound. Appl. Mech. Rev., vol. 35, no. 8, Aug. 1982, pp. 1047-1057.
7. Fu, L.S.: On Ultrasonic Factors and Fracture Toughness. Eng. Fract. Mech., vol. 18, no. 1, 1983, pp. 59-67.
8. Fu, L.S.: Micromechanics and its Application to Fracture and NDE. Developments in Mechanics, Vol. 12, E.J. Haug and K. Rim, eds., University of Iowa Press, 1983, pp. 263-265.
9. Generazio, E.R.: The Role of The Reflection Coefficient in Precision Measurement of Ultrasonic Attenuation. Mater. Eval., vol. 43, no. 8, July 1985, pp. 995-1004.
10. Green, R.E., Jr.: Ultrasonic Investigation of Mechanical Properties. Treatise on Materials Science and Technology, Vol. 3, Academic Press, 1973.

11. Green, R.E., Jr.: Non-Linear Effects of High Power Ultrasonics in Crystalline Solids. Ultrasonics, vol. 13, no. 3, May 1975, pp. 117-127.

12. Green, R.E., Jr.: Effect of Metallic Microstructure on Ultrasonic Attenuation. Nondestructive Evaluation: Microstructural Characterization and Reliability Strategies, O. Buck and S.M. Wolf, eds., The Metallurgical Society of AIME, 1981, pp. 115-132.

13. Green, R.E., Jr.: Ultrasonic Nondestructive Materials Characterization. Analytical Ultrasonics in Materials Research and Testing, NASA CP-2383, 1986, pp. 1-30.

14. Hahn, G.T.; Kanninen, M.F.; and Rosenfield, A.R.: Fracture Toughness of Materials. Annual Reviews of Materials Sceince, Vol. 2, R.A. Huggins, ed., Annual Reviews Inc., 1972, pp. 381-404.

15. Kanninen, M.F.; and Popelar, C.H.: Advanced Fracture Mechanics, Oxford University Press, 1985.

16. Kolsky, H.: Stress Waves in Solids, Dover Publishers, 1963.

17. Kolsky, H.: Recent Work on the Relations Between Stress Pulses and Fracture. International Conference on Dynamic Crack Propagation, G.C. Sih, ed., Noordhoff, 1972, pp. 399-414.

18. MacCrone, R.K., ed.: Properties and Microstructure. Treatise on Materials Science and Technology, Vol. 11. Academic Press, 1977.

19. Mignogna, R.B.; and Green, R.E., Jr.: Effects of High Frequency Loading on Materials. Ultrasonic Fatigue, J.M. Wells, O. Buck, L.D. Roth, and J.K. Tien, eds., The Metallurgical Society of AIME, 1982, pp. 63-85.

20. Nowick, A.S.; and Berry, B.S.: Anelastic Relaxation in Crystalline Solids, Academic Press, 1972.

21. Papadakis, E.P.: Ultrasonic Velocity and Attenuation: Measurement Methods With Scientific and Industrial Applications. Physical Acoustics - Principles and Methods, Vol. 12, W.P. Mason and R.N. Thurston, eds., Academic Press, 1976, pp. 277-374.

22. Sachse, W.; and Green, R.E., Jr.: Deformation Rate Effects on the Attenuation During Loading, Unloading, and Reloading of Aluminum Crystals. J. Phys. Chem. Solids, vol. 31, no. 8, Aug. 1970, pp. 1955-1961.

23. Serabian, S.; and Williams, R.S.: Experimental Determination of Ultrasonic Attenuation Characteristics Using the Roney Generalized Theory. Mater. Eval., vol. 36, no. 8, July 1978, pp. 55-62.

24. Serabian, S.: Frequency and Grain Size Dependency of Ultrasonic Attenuation in Polycrystalline Materials. Brit. J. Nondestr. Test., vol. 22, no. 2, Mar. 1980, pp. 69-77.

25. Truell, R.; Elbaum, C.; and Chick, B.B.: Ultrasonic Methods in Solid State Physics. Academic Press, 1969.

26. Vary, A.: Correlations Among Ultrasonic Propagation Factors and Fracture Toughness Properties of Metallic Materials. Mater. Eval., vol. 36, no. 7, June 1978, pp. 55-64.

27. Vary, A.: Correlations Between Ultrasonic and Fracture-Toughness Factors in Metallic Materials. Fracture Mechanics, C.W. Smith, ed., ASTM STP-677, American Society for Testing and Materials, 1979, pp. 563-580.

28. Vary, A.: Computer Signal Processing for Ultrasonic Attenuation and Velocity Measurements. Proceedings of the Twelfth Symposium on Nondestructive Evaluation, W.W. Bradshaw, ed., American Society for Nondestructive Testing, 1979, pp. 33-46.

29. Vary, A.: Ultrasonic Measurement of Material Properties. Research Techniques in Nondestructive Testing, Vol. 4, R.S. Sharpe, ed., Academic Press, 1980, 159-204.

30. Vary, A.: Concepts and Techniques for Ultrasonic Evaluation of Material Mechanical Properties. Mechanics of Nondestructive Testing, W.W. Stinchcomb, ed., Plenum Publishing Co., 1980, pp. 123-141.

31. Vary, A.: Fundamentals of Ultrasonic NDE for Microstructure/Material Property Interrelations. Advanced Materials Technology, NASA CP-2251, 1982, pp. 411-420.

32. Vary, A.; and Bowles, K.J.: Ultrasonic Evaluation of the Strength of Unidirectional Graphite-Polyimide Composites. Proceedings of the Eleventh Sympodium on Nondestructive Evaluation, American Society for Nondestructive Testing, 1977, pp. 242-258.

33. Vary, A.; and Hull, D.R.: Interrelation of Material Microstructure, Ultrasonic Factors, and Fracture Toughness of a Two-Phase Titanium Alloy. Mater. Eval., vol. 41, no. 3, Mar. 1983, pp. 309-314.

34. Vary, A.; and Hull, D.R.: Ultrasonic Ranking of Toughness of Tungsten Carbide. NASA TM-83358, 1983.

35. Vary, A.; and Lark, R.F.: Correlation of Fiber Composite Tensile Strength With the Ultrasonic Stress Wave Factor. J. Test. Eval., vol. 7, no. 4, July 1979, pp. 185-191.

36. Vary, A.; and Kautz, H.E.: Transfer Function Concept for Ultrasonic Characterization of Material Microstructures Analytical Ultrasonics in Research and Testing, NASA CP-2383, 1986, pp. 257-298.

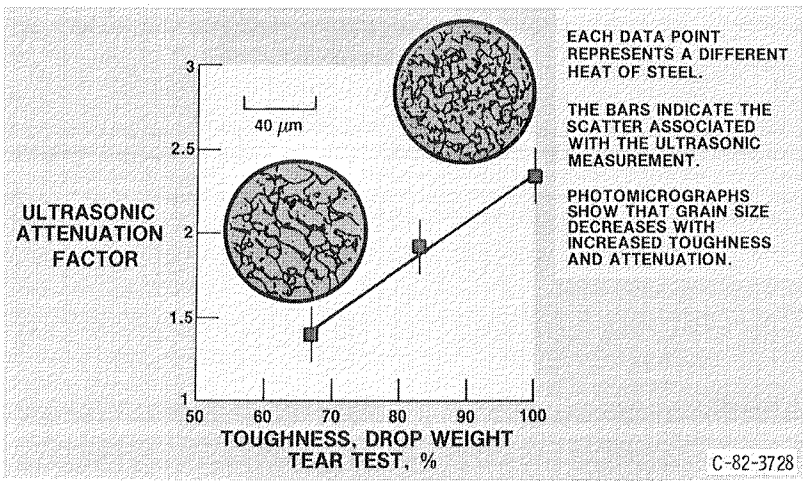

Figure 1. - Ultrasonic attenuation factor as function of toughness as measured by drop weight test for low carbon steel (Vary, 1982).

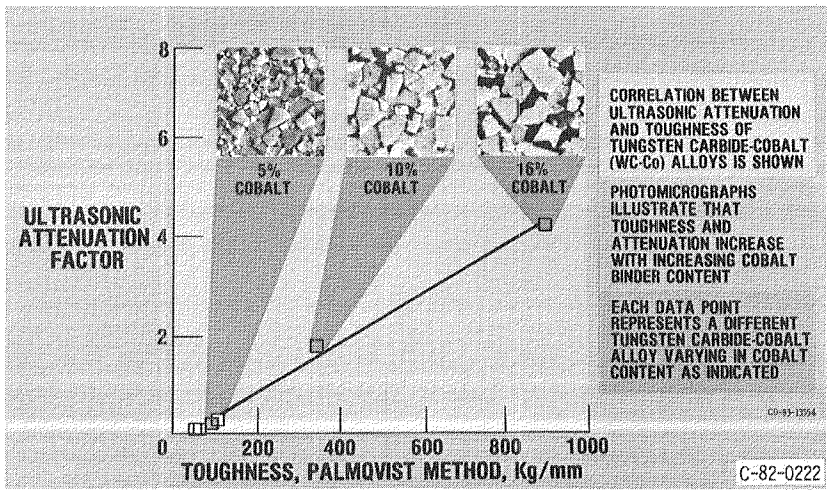

Figure 2. - Ultrasonic attenuation factor as function of toughness as measured by Palmqvist method for cobalt cemented tungsten carbide (Vary and Hull, 1983).

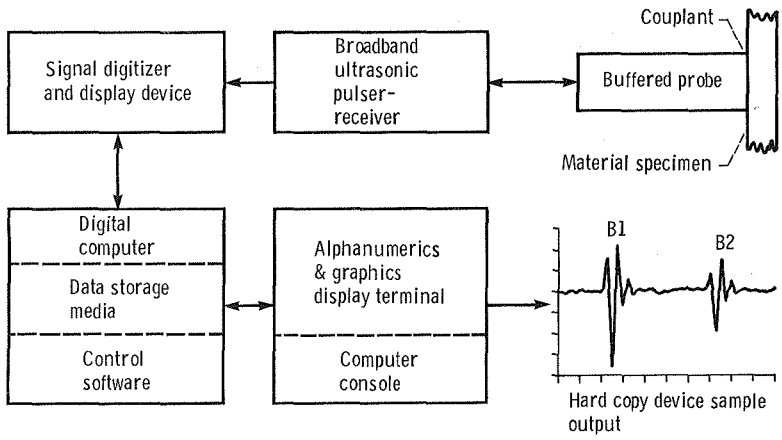

Figure 3. - Block diagram of computer system for ultrasonic signal acquisition and processing for pulse-echo velocity and attenuation measurements. Probe is both transmitter and receiver.

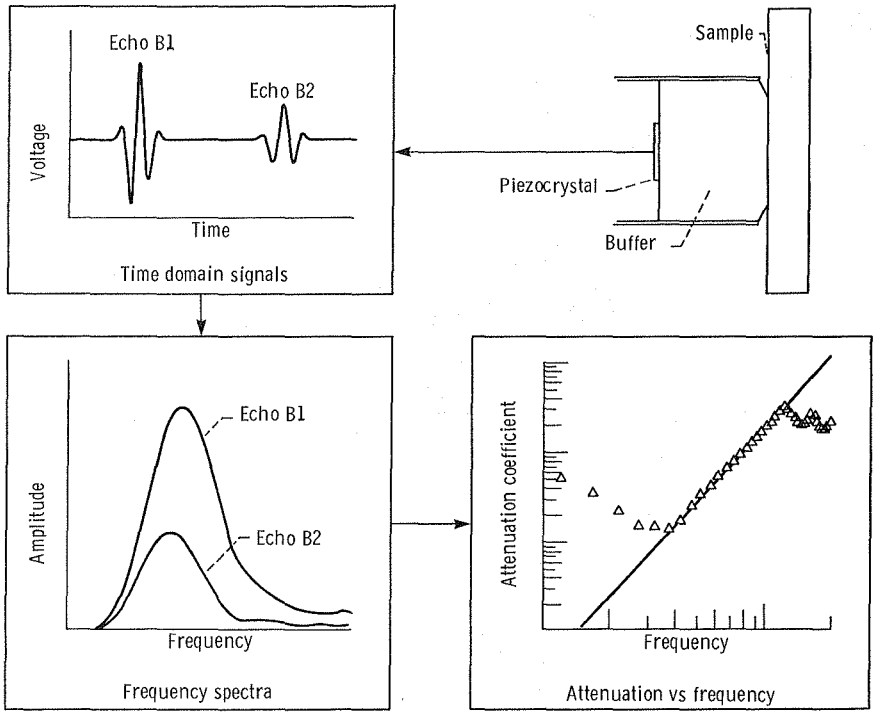

Figure 4.- Illustration of ultrasonic signal processing procedure for attenuation measurements using pulse-echo method.

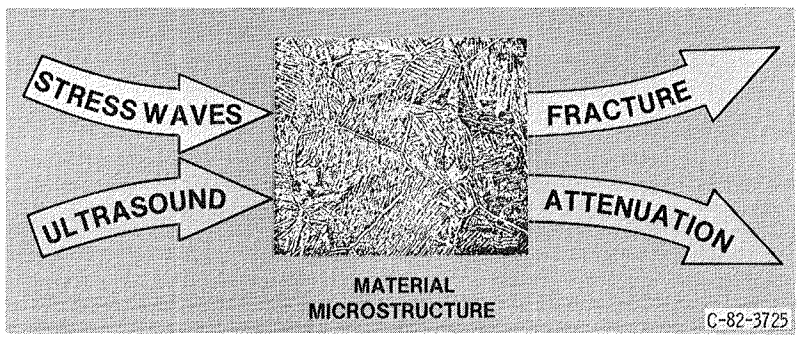

Figure 5. - Diagram of concept wherein ultrasonic attenuation measures microstructural factors that govern stress wave propagation during microfailure events.

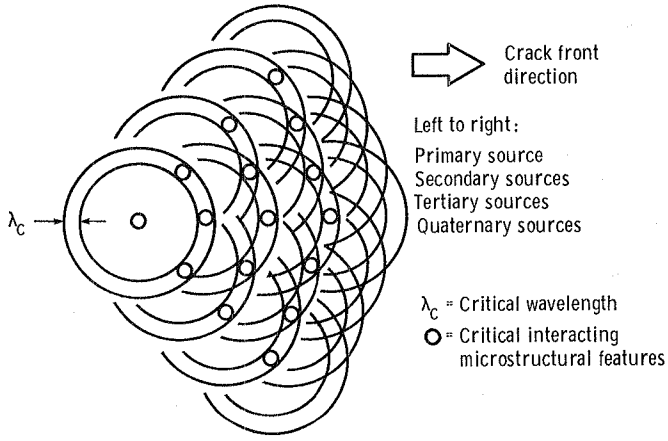

Figure 6. - Diagram illustrating stress wave interaction (SWI) model showing cascade effect during interactions with critical microstructural features.

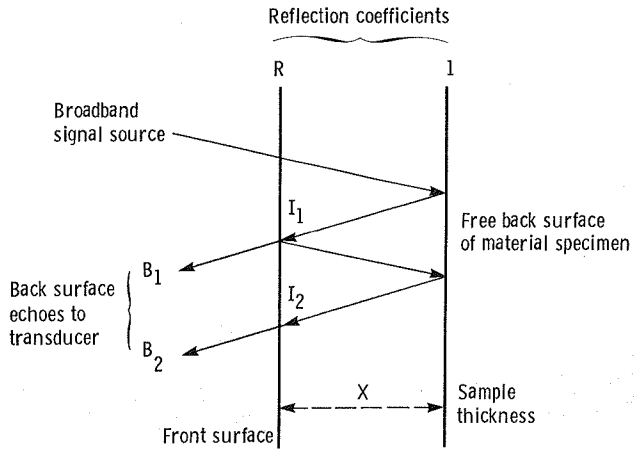

Figure 7. - Diagram of echo system for defining the microstructure transfer function (MTF).

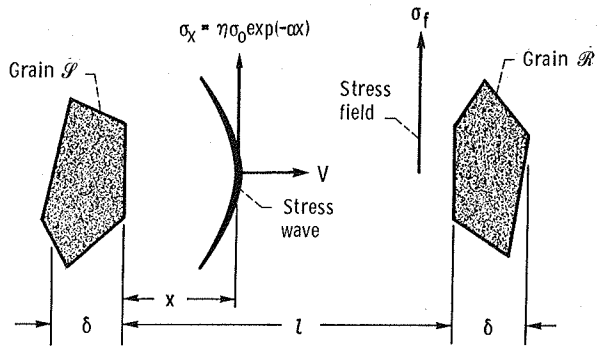

Figure 8. - Diagram of microcrack nucleation mechanics (MNM) model wherein crack nucleation in grain $\mathscr{S}$ produces crack nucleation in grain $\mathscr{R}$ via stress wave interaction. (η is a geometric factor).

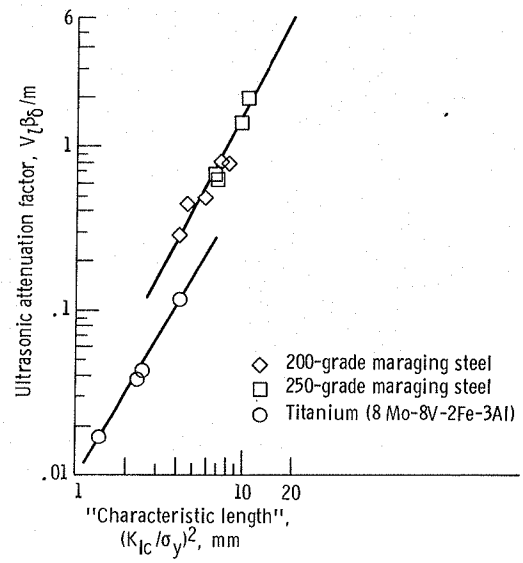

Figure 9. - Experimental results showing predicted correlation of ultasonic attenuation factor and fracture toughness (characteristic length) factor, (Vary, 1978; 1979a).

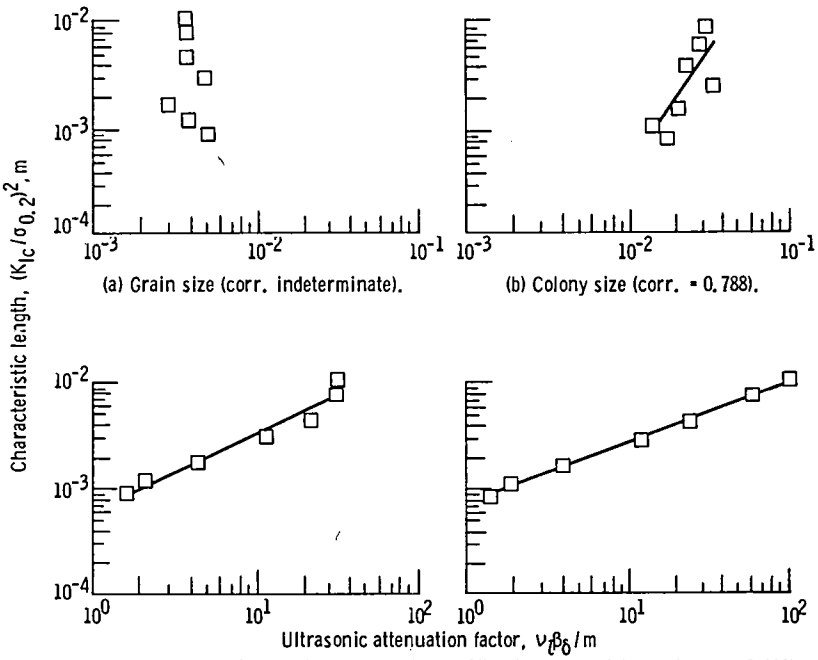

(a) Grain size (corr. indeterminate).

(b) Colony size (corr. = 0.788).

(c) Alpha phase thickness (corr. = 0.977).

(d) Beta phase thickness (corr. = 0.998).

Figure 10.- Comparison of toughness (characteristic length) and attenuation factors for four microstructural features in a two-phase titanium alloy (Vary and Hull, 1982). ($\sigma_{0.2}$ = yield strength at 0.2% offset).

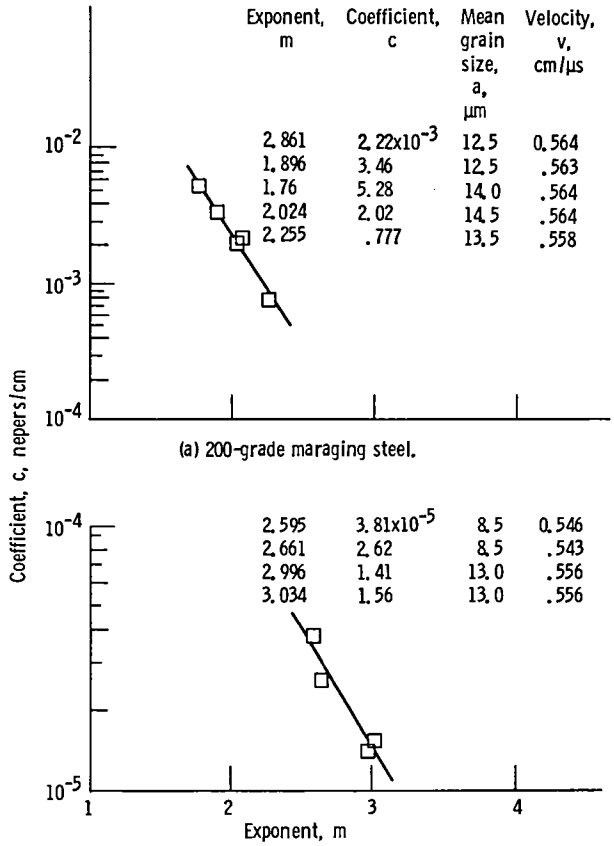

(a) 200-grade maraging steel.

(b) 250-grade maraging steel.

Figure 11. - Interdependence of the experimentally determined attenuation parameters c and m for two maraging steels, equation (7) (Vary and Kautz, 1986).

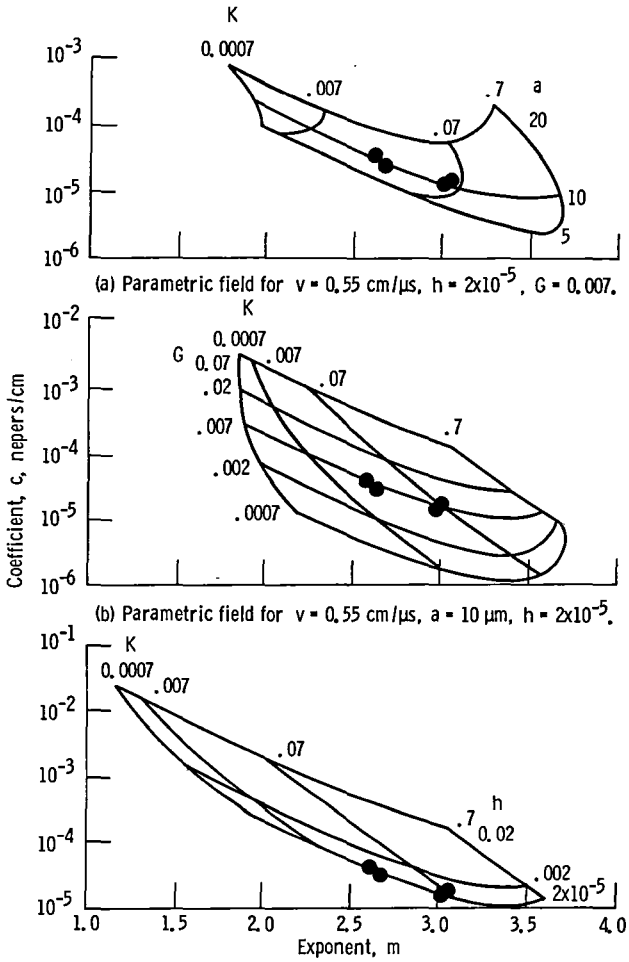

(a) Parametric field for v = 0.55 cm/μs, h = $2x10^{-5}$, G = 0.007.

(b) Parametric field for v = 0.55 cm/μs, a = 10 μm, h = $2x10^{-5}$.

(c) Parametric field for v = 0.55 cm/μs, a = 10 μm, G = 0.007.

Figure 12. - Parametric fields of c versus m based on equations (6) and (7) for assigned values of mean grain size, a, boundary reflection coefficient, G, damping constant, h, elastic anisotropy, K, and velocity, v. Data for 250 grade maraging steel from figure 11, are co-plotted within the fields. (Vary and Kautz, 1986).

1. Report No.	2. Government Accession No.	3. Recipient's Catalog No.
NASA TM-87339		

4. Title and Subtitle	5. Report Date
Concepts for Interrelating Ultrasonic Attenuation, Microstructure, and Fracture Toughness in Polycrystalline Solids	May 1986
	6. Performing Organization Code: 506-53-1A
7. Author(s): Alex Vary	8. Performing Organization Report No: E-3086
	10. Work Unit No
9. Performing Organization Name and Address: National Aeronautics and Space Administration, Lewis Research Center, Cleveland, Ohio 44135	11. Contract or Grant No.
	13. Type of Report and Period Covered: Technical Memorandum
12. Sponsoring Agency Name and Address: National Aeronautics and Space Administration, Washington, D.C. 20546	14. Sponsoring Agency Code

15. Supplementary Notes

Material previously presented at the Symposium on Solid Mechanics Research for Quantitative NDE, sponsored by the Office of Naval Research, held at Northwestern University, Evanston, Illinois, September 18-20, 1985.

16 Abstract

Conceptual models are advanced for explaining and predicting empirical correlations found between ultrasonic measurements and fracture toughness of polycrystalline solids. The models lead to insights concerning microstructural factors governing fracture processes and associated stress wave interactions. Analysis of the empirical correlations suggested by the models indicates that, in addition to grain size and shape, grain boundary reflections, elastic anisotropy, and dislocation damping are factors that underly both fracture toughness and ultrasonic attenuation. One outcome is that ultrasonic attenuation can predict the size of crack blunting or process zones that develop in the vicinity active cracks in metals. This forms a basis for ultrasonic ranking according to variations in fracture toughness.

17 Key Words (Suggested by Author(s))	18 Distribution Statement
Nondestructive testing/evaluation; Ultrasonics; Ultrasonic attenuation; Fracture toughness; Polycrystalline metals; Microstructure	Unclassified - unlimited STAR Category 38

19 Security Classif. (of this report)	20. Security Classif. (of this page)	21. No. of pages	22. Price*
Unclassified	Unclassified		

*For sale by the National Technical Information Service, Springfield, Virginia 22161

End of Document